doi:10.1006/mthe.2002.0600, available online at http://www.idealibrary.com on IDEAL

Determinants of Hepatitis C Translational Initiation *in Vitro*, in Cultured Cells and Mice

Anton P. McCaffrey,[1] Kazuo Ohashi,[1] Leonard Meuse,[1] Shiliang Shen,[1] Alissa M. Lancaster,[2] Peter J. Lukavsky,[3] Peter Sarnow,[3] and Mark A. Kay[1,*]

[1]*Program in Human Gene Therapy, Departments of Pediatrics and Genetics,* [2]*Department of Microbiology and Immunology, and* [3]*Department of Structural Biology, Stanford University School of Medicine, Stanford, California 94305, USA*

**To whom correspondence and reprint requests should be addressed. Fax: (650) 498-6540. E-mail: Markay@stanford.edu.*

Hepatitis C virus (HCV) is an RNA virus infecting 1 in every 40 people worldwide. Development of new therapeutics for treating HCV has been hampered by the lack of small-animal models. We have adapted existing hydrodynamic transfection methods to optimize the delivery of RNAs to the cytoplasm of mouse liver cells *in vivo*. Transfected HCV genomic RNA failed to replicate in mouse liver, suggesting a post-entry block to viral replication. Real-time imaging of HCV internal ribosome entry site (IRES) firefly luciferase reporter mRNA translation in living mice demonstrated that the HCV IRES was functional in mouse liver. We then used this system as a model for studying HCV RNA translation in mice. We compared translation by several mutant HCV IRES variants in cell lysates, cultured cells, and mouse liver. We measured the contribution to translation of a cap, HCV 3′-untranslated region (UTR), poly(A) tail, domains II, IIIb, IIIabc, IIIabcd, IIId, and the initiator codon. Efficient translation required a 3′-UTR in mice and HeLa cells, but not in rabbit reticulocyte lysates. Translational regulation of transfected RNAs was stringent in mice. The method we describe could be useful for studies in mice of antisense or ribozyme inhibitors targeting the IRES as well as other RNA biochemical studies *in vivo*.

Key Words: ribosome, RNA transfection, hydrodynamic transfection, RNA localization, cell lysates, diagnostic imaging, animal disease model

INTRODUCTION

Hepatitis C virus (HCV) is a positive-strand RNA virus that infects 170 million people worldwide [1] and is the most common reason for liver transplantation in the western world [2]. Current treatments for HCV (interferon or interferon and ribavirin) are not very effective and result in elimination of the virus in only 20–40% of patients [2]. New treatments for HCV are urgently needed.

Translation of the HCV polyprotein initiates at a highly structured internal ribosome entry site (IRES) at the 5′ end of the genomic RNA. The 3′-untranslated region (UTR) of HCV also contains an unusual and highly structured region, termed the 3′ X region [3,4], that may influence translational regulation from the IRES [5]. It has been proposed that the highly conserved 5′- [6] and 3′-UTRs [3] would be good targets for therapeutic intervention. Extensive effort has been devoted to the development of antisense oligonucleotides and ribozyme inhibitors targeting the conserved HCV IRES sequence [7]. However, testing of these nucleic acid inhibitors *in vivo* has been hampered by the lack of a convenient small-animal model for HCV IRES function. Recently, a mouse xenotransplantation model was reported that supports HCV viral replication in transplanted human liver cells [8]. While very exciting, this system requires access to fresh human liver tissue. So far, no small-animal model amenable to high-throughput screening of HCV IRES inhibitors has been described.

Cell extract and cell culture translation assays have been invaluable for studies of translational initiation at the HCV IRES. They have been used to map the IRES 5′ and 3′ boundaries, to identify essential sequences and secondary structures, and to identify protein-binding sites within the IRES [reviewed in 9,10]. Specific domains in the IRES contribute to its translational activity both *in vitro* and in cell culture assays. However, conflicting results from different reports are difficult to reconcile because of differences in the model systems used by the various researchers. There are several reports that cell culture assays have more stringent requirements for efficient translation than cell lysate assays [11,12]. The type of lysate or cell line used [12], the concentration of salts in cell lysates [10,12],

1525-0016/02 $35.00

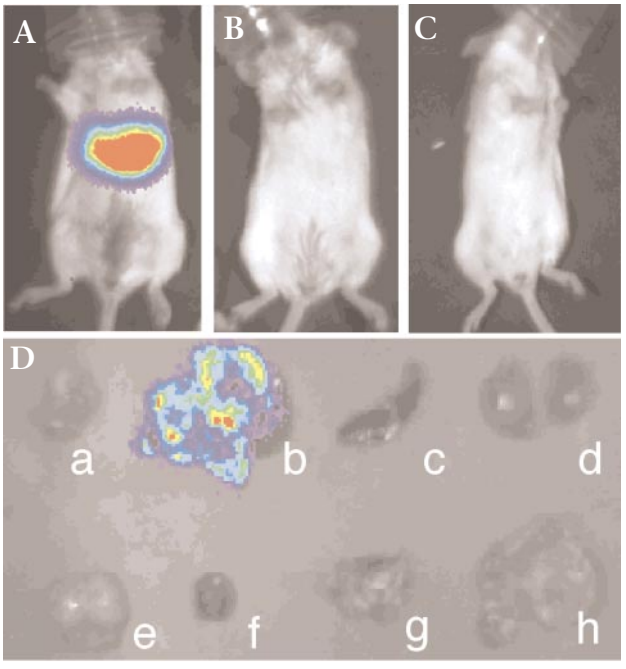

FIG. 1. *In vivo* imaging of luciferase activity. Light emitted as a result of *in vivo* luciferase activity from expressed protein was used to monitor hydrodynamic luciferase RNA transfection. RNAs were mixed with 400 units of native RNasin (Promega), competitor RNA (to give 80 μg total nucleic acid), 2 ml of 25°C PBS, and injected under high pressure into the tail veins of mice over 4–5 seconds. After 3 hours, luciferin (the substrate of luciferase) was injected i.p., and living animals were imaged under general anesthesia 10 minutes later using a CCD camera as described [25]. (A) Light emitted from a mouse receiving 50 μg of luciferase RNA demonstrated that hydrodynamic RNA transfection resulted in transfer to and expression of RNA in the liver. (B) No light was detected from a mouse that received 2.5 μg of SP6 control DNA (the transcription template for luciferase RNA). (C) No light was detected from a mouse that received 50 μg of luciferase RNA that had been incubated with 1500 units RNase T1 (Life Technologies, Rockville, MD) for 30 minutes at 37°C. The results in (B) and (C) demonstrate that light emission in (A) was not due to DNA contamination. (D) Muscle (a), liver (b), spleen (c), kidneys (d), brain (e), heart (f), lung (g), and intestine (h) of a mouse that received 50 μg of luciferase RNA. Liver was the only organ with detectable luciferase expression at 3 hours, other than the tail (injection site).

and the transcriptional start sequence may also influence translational readout [13]. A recent report that HCV IRES translation varies with cell cycling [14] also raises concern that rapidly dividing cells in tissue culture may not accurately model the translation of viral proteins in the normally quiescent human liver [15,16]. Differences between *in vitro* and cell culture assays led Kamoshita *et al.* to suggest that an *in vivo* method to measure HCV IRES activity in tissues would be desirable [12]. A comprehensive comparison of IRES function in cell lysates, in cultured cells, and in the liver of a small animal has not been conducted.

These concerns prompted us to develop a mouse model to study translation from the HCV IRES in living mice. To accomplish this, we adapted previously described hydrodynamic transfection methods [17–21] to transfer RNAs efficiently to the livers of living mice. We used fusion RNAs containing the HCV IRES driving translation of luciferase protein to investigate the following questions. Can HCV RNA replicate in mouse liver? Is the HCV IRES functional in mouse liver? Does the HCV 3′-UTR (or the poly(A) used by cellular mRNAs) affect translation from the HCV IRES? What are the effects on translation of deletions and substitutions within the IRES? We then compared translational measurements in mice to those in rabbit reticulocyte lysates (RRL) and HeLa cells.

RESULTS

Transfer of Functional RNA to the Livers of Mice

High-pressure injection of naked DNA into the tail vein of rodents leads to efficient transgene expression in the liver [17–20]. Modest transfection of muscle cells by direct injection of luciferase RNA has also been reported [22]. Chang *et al.* reported that hydrodynamic transfection of hepatitis delta virus (HDV) DNAs or RNAs into mice led to initiation of a viral replication cycle [21]. This demonstrated that naked RNA injection was a viable method for initiating a viral replication cycle; however, parameters for achieving high-level RNA transfection were not elucidated. One goal of our studies was to establish the important variables required to achieve efficient transfer of RNA to the livers of living mice. We monitored expression of the RNA by whole-body imaging of *in vivo* luciferase activity, a method that has previously been used to monitor tumor cell proliferation [23], bacterial infection [24], *in vivo* DNA transfer, and gene expression [25] in living mice.

We injected luciferase-encoding RNAs either with no RNase inhibitor or in combination with various amounts of RNase inhibitor or competitor RNA into mice. We used light transmitted through the tissues of treated animals as a measure of luciferase enzyme activity. We mixed 50 mg of 7-methylguanosine-capped and polyadenylated RNA coding for the luciferase gene with the ribonuclease inhibitor, RNasin, as well as an uncapped, non-polyadenylated competitor RNA (compRNA), and injected the mixture into the tail veins of mice. Figure 1A shows an image of light emitted from a mouse 3 hours after RNA injection; considerable levels of luciferase activity can be observed in a discrete location in the animal. This image consisted of a pseudocolor pattern representing intensity of emitted light (red most and blue least intense), superimposed on a gray-scale reference background image of the animal (for orientation).

To exclude the unlikely possibility that the observed luciferase activity was the result of DNA contamination, we injected two control preparations into mice. The first control contained 2.5 μg of linearized template DNA for luciferase RNA transcription (equivalent to the DNA used to generate 50 μg of luciferase RNA). Even if the template DNA survived DNase I treatment and purification on a silica membrane (removes DNA), it does not contain a

doi:10.1006/mthe.2002.0600, available online at http://www.idealibrary.com on IDEAL

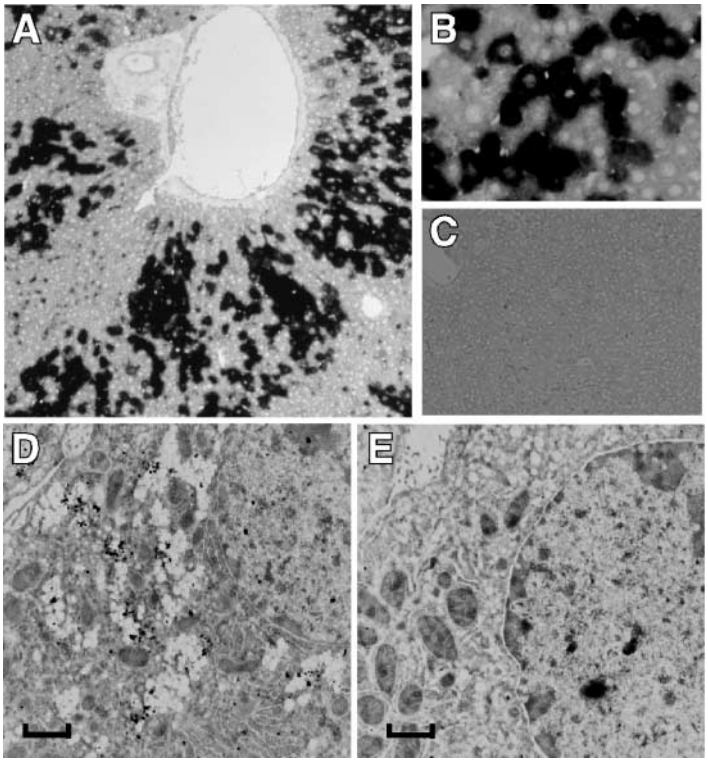

FIG. 2. Subcellular localization of transfected RNAs. Digoxigenin-labeled probes were visualized with anti-digoxigenin antibodies conjugated to 1-nm gold particles followed by silver enhancement. Each probe contains multiple digoxigenin labels. In all *in situ* experiments, 50 μg of luciferase RNA was mixed with 30 μg of competitor RNA, 800 units of RNasin, and injected. Livers were fixed at 15 minutes postinjection for *in situ* hybridization. (A, B) Positive immunohistochemical staining of luciferase RNA with antisense probe. Stained RNA is observed predominantly in the cytoplasm. A total of 15 fields from two sections were counted, and ~ 33.4% (± 2.5%) of cells were stained. (C) No immunohistochemical staining is seen with sense probe (that should not recognize luciferase RNA). (D, E) Electron microscopy of liver sections. Closely spaced groups of particles representing positive staining with antisense probe (D) were seen free within the cytoplasm and not visualized within endosomes or in the nucleus. Only background staining (rare individual particles) was seen with sense probe (E). Original magnification: (A, C) ×100; (B) ×400.

eukaryotic promoter and thus should not be transcribed in mice. The second control consisted of 50 μg of luciferase RNA that was pretreated with RNase T1, which should degrade the luciferase RNA but not contaminating DNA. We repurified the sample to remove the RNase T1. Luciferase activity was not detected in mice that received either control preparation (Figs. 1B and 1C, respectively; $n = 3$ for each group). These data show that hydrodynamic RNA transfection in the presence of RNasin and competitor RNA leads to RNA transfer and subsequent translation *in vivo*. In this model system, RNasin was absolutely required for detectable luciferase activity.

Localization of Hydrodynamically Transfected RNAs

The method by which hydrodynamically transfected DNA enters cells remains controversial, although it has been proposed that entry might occur via receptor-mediated endocytosis [26]. If a specific receptor is required for cell entry, it is not clear that transfected RNAs and DNAs would have the same localization. Alternatively, DNA may enter cells by transient disruption of the cell membrane as the result of external pressure [26]. If this is the case, one might expect that hydrodynamically transfected RNAs and DNAs would be localized to the same tissues and subcellular compartments. To clarify this issue, we employed whole-organ imaging as well as *in situ* hybridization to examine the localization of hydrodynamically transfected RNAs.

To identify the organs targeted by hydrodynamic RNA transfection, we injected 50 μg of luciferase RNA. We injected luciferin intraperitoneally (i.p.) 3 hours postinjection; the mouse was killed 10 minutes later and its internal organs imaged. Luciferase activity was detectable in the liver and injection site, but not in any other tissue analyzed (muscle, spleen, kidneys, intestine, lung, heart, and brain) (Fig. 1D). Because luciferin has been shown to gain access to many tissues when injected i.p. [25], these results demonstrate that hydrodynamic RNA transfection leads to substantial RNA transfection of primarily the liver.

To determine the subcellular localization of injected RNAs, we conducted *in situ* hybridization on liver sections at the level of light microscopy (Figs. 2A, 2B, and 2C) and electron microscopy (Figs. 2D and 2E). Specific staining in the cytoplasm with an antisense probe was seen in 33% (± 2.5%) of mouse hepatocytes and nonparenchymal cells (Figs. 2A and 2B), with no staining using a sense RNA probe (Fig. 2C). Standard transfection methods frequently result in RNA entrapment in endosomal compartments [27]. Using electron microscopy, we observed considerable levels of hybridization (groups of particles bound to multiple digoxigenin molecules within each probe) exclusively within the cytoplasm of transfected cells using an antisense probe (Fig. 2D). No hybridization occurred with a sense probe used in a control experiment (Fig. 2E). Collectively, these results show that hydrodynamic RNA transfection can efficiently target considerable amounts of RNA to the cytoplasm of mouse liver cells, with the desired subcellular localization for HCV RNAs. The almost immediate appearance of free RNA in the cytoplasm argues against receptor-mediated endocytosis and for transient membrane disruption.

Amount of Emitted Light Is Dependent on Dose of Coinjected RNasin, the Presence of Competitor RNA, and the Dose of Luciferase RNA

We conducted two experiments to determine further the dependence of luciferase activity on the amount of injected RNasin, competitor RNA, and luciferase RNA. We

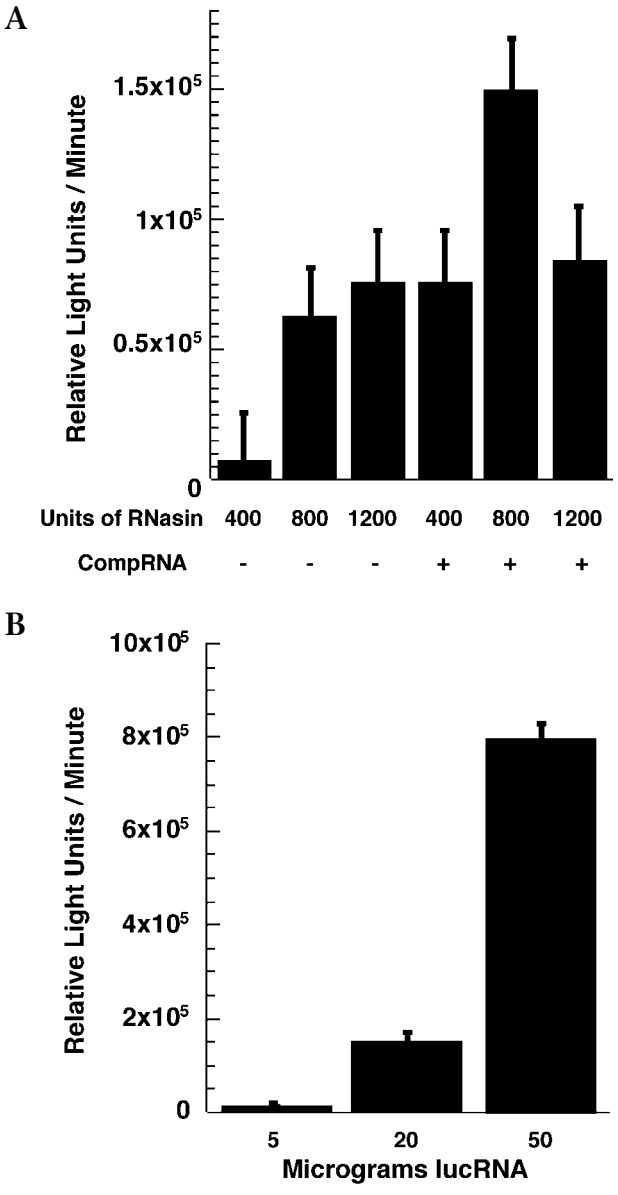

FIG. 3. Transfection depends on RNasin dose and luciferase RNA dose and the presence of competitor RNA. Signal intensity reflects amount of injected RNA. (A) Relative light units per minute emitted from animals that were injected with 20 μg of luciferase RNA and 400, 800, or 1200 units of RNasin with or without 60 μg of competitor RNA. Animals were imaged at 3 hours ($n = 3$). In the absence of competitor RNA, increasing RNasin doses gave increased luciferase activity. In the presence of competitor RNA, 800 and 1200 units of luciferin gave comparable activity that was greater than with 400 units. (B) Relative light units emitted from mice injected with 5, 20, or 50 μg of luciferase RNA and 60 μg of competitor RNA. Animals ($n = 5$, 5, and 6 for groups receiving 5, 20, and 50 μg of RNA, respectively) were imaged at 3 hours postinjection. Error bars indicate SEM calculated for each group. Increasing doses of luciferase RNA gave increasing luciferase activity.

injected luciferase RNA into mice without RNasin or in the presence of various amounts of RNasin with or without 60 μg of uncapped, unpolyadenylated competitor RNA (Fig. 3A; $n = 3$ per group). In the absence of RNasin, there was no detectable luciferase expression ($n = 4$), even using a camera that is ~ 100-fold more sensitive than the instrument used to collect the original data. In the absence of competitor RNA, increased amounts of RNasin (between 400 and 1200 units) gave increased luciferase expression. At all doses of RNasin, inclusion of competitor RNA increased luciferase expression. In the presence of competitor RNA, 800 units of RNasin resulted in more intense signals than 400 units, and the signal intensity was comparable to that observed with 1200 units. RNasin and competitor RNA presumably protect luciferase RNA *in vivo* by competitively binding RNases present in the bloodstream and extracellular space. It is unclear whether RNasin alters intracellular RNA stability, although RNasin added to injected luciferase plasmids did not increase expression from these DNAs (data not shown). Another dose experiment with 5, 20, and 50 μg of luciferase RNA (Fig. 3B; $n = 5$, 5, and 6 for groups receiving 5, 20, and 50 μg of RNA, respectively) demonstrated a dose-dependent increase in luciferase activity.

Rate of Decay of Luciferase Activity Sets a Limit on Luciferase Half-Life

We monitored changes in luciferase expression every 3 hours after *in vivo* RNA delivery ($n = 5$ for 3-hour time point and $n = 6$ for 6-, 9-, and 12-hour time points). Analyses of light emission in treated mice showed exponential RNA decay *in vivo*, with an apparent rate constant of 0.3 h^{-1} (Fig. 4). Working with these results, we estimated an upper limit for the $t_{1/2}$ of luciferase protein in the liver to be ~ 2.3 hours. This is shorter than the $t_{1/2}$ estimations of 3 hours obtained in cell culture studies [28]. This may reflect differences in protein stability in the cultured cells used compared with mouse hepatocytes. These results demonstrate that hydrodynamic RNA transfection can be used to estimate protein half-lives in mice.

Transduced HCV Genomic RNAs Do Not Replicate in Mouse Liver

Currently, primates are the only mammals that have been shown to support replication of HCV. Kolykhalov *et al.* showed that HCV genomic RNAs made *in vitro* were infectious and caused disease in chimpanzees after direct intrahepatic inoculation [29]. A replication-defective genomic RNA with an in-frame deletion in the NS5B polymerase was used as a negative control. Inoculation of mice with infectious HCV particles does not lead to a viral replication cycle (data not shown). It is unclear whether this result is due to a lack of a receptor for HCV internalization on the surface of mouse hepatocytes, or due to a block in replication that occurs after internalization.

doi:10.1006/mthe.2002.0600, available online at http://www.idealibrary.com on IDEAL

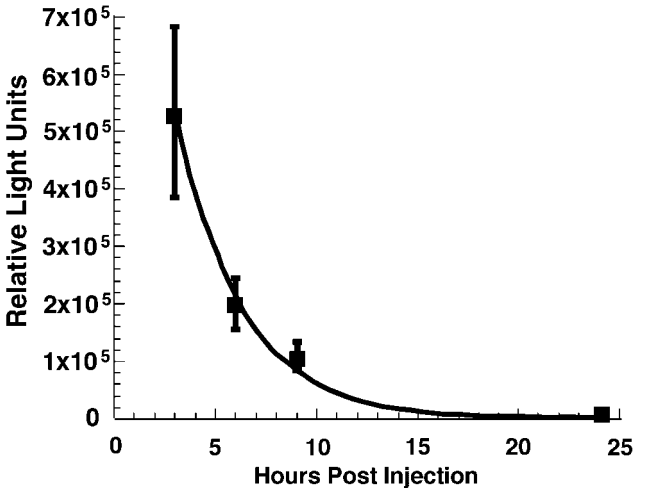

FIG. 4. *In vivo* kinetic measurement of luciferase protein half-life in mice. A mixture of 20 μg of luciferase RNA, 60 μg of competitor RNA, and 800 units of RNasin was injected into mice ($n = 5$ for 3-hour time point and $n = 6$ for 6-, 9-, and 12-hour time points). Error bars indicate SEM calculated for each group. Data were fitted to a first-order exponential equation by linear regression to yield an apparent rate constant of 0.3 h^{-1}.

We next determined if bypassing the internalization step by transfection of mouse liver with HCV genomic RNA would lead to RNA replication. HCV genomic RNA or RNA containing inactivating substitutions in NS5B (rep⁻ RNA) were injected into mice. Mixtures containing 40 μg of genomic (or rep⁻ RNA), 40 μg of a capped polyadenylated RNA encoding human factor IX (FIX RNA), 40 μg competitor RNA, and 800 units of RNasin were hydrodynamically injected into NOD/LtSz-*Prkdcscid* mice. We measured serum FIX levels by ELISA 3 hours after injection and used them to correct for RNA transduction efficiency. At various times, animals were killed and RNA was extracted from serum and liver for analysis. We then used quantitative RT-PCR to measure HCV and mouse glyceraldehyde 3-phosphate dehydrogenase (GAPD) levels in these samples (normalized values = (HCV RNA/GAPD)/FIX). Figure 5 shows the decay of HCV genomic RNA and rep⁻ RNA in mouse liver. Both RNAs decay with similar $t_{1/2}$ values of ~ 22 hours, suggesting that replication of the genomic RNA does not occur in mouse liver. Serum measurements of genomic RNA and rep⁻ RNA at various times were also similar (data not shown). It is clear from the data in Figures 1 and 2 that hydrodynamically transfected RNA reached the cytoplasm of hepatocytes and was functional. Taken together, our data suggest that there was a post-entry block to HCV replication in mice. We next used hydrodynamic RNA transfection to examine the functionality of the HCV 5′- and 3′-UTR in mouse liver, and to compare these results with reported data from standard *in vitro* and culture models.

Translational Efficiency of IRES and 3′-End Variants of Luciferase Fusion RNAs Studied in Mice, HeLa Cells, and RRLs

Considerable effort is being devoted to the identification of potential inhibitors of different steps in the HCV life cycle. However, before candidate inhibitors such as antisense oligonucleotides and ribozymes can be tested in humans, preclinical small-animal model systems will be required to assess their safety and efficacy. Preliminary studies showed that transfection of both luciferase mRNAs containing or lacking the 5′-UTR of HCV led to emission of light in the liver of transfected mice. This finding demonstrated for the first time that the HCV IRES was functional in mouse liver (data not shown). This finding indicates that hydrodynamic RNA transfection could be used to test potential translational inhibitors for biochemical studies of IRES function in mice. However, such a system would only be useful if proper translational regulation of the IRES was maintained. To assess translational regulation in this novel mouse model system, we compared the translational efficiencies of several IRES variants in mice with standard *in vitro* model systems such as HeLa cells and RRLs. Although none of these model systems completely recapitulates HCV translation in an infected human liver, hydrodynamic RNA transfection provides the opportunity, for the first time, to monitor HCV translational regulation within an intact organ (the liver).

A number of groups have reported differences between *in vitro* and cell culture measurements of HCV IRES variant activities [5,11,12]. There are also conflicting reports as to the effect of a cap on IRES activity [30,31], and the effect of the HCV 3′-UTR on translation remains unclear [5,32]. Therefore, we conducted a comparative analysis of IRES translation in nuclease-treated RRLs, HeLa cells, and mice (Fig. 6).

Effect of 5′ Cap and HCV 3′-UTR or 3′ Poly(A) on Translation

Studies of cap-dependent translation in yeast and RRLs have suggested that interactions between cap-binding proteins and poly(A)-binding protein circularize mRNAs and enhance translation in eukaryotes [reviewed in 33]. It has also been suggested [5,32] that proteins bound to the IRES and the HCV 3′-UTR might circularize the HCV genomic RNA and thereby regulate translation. To assess the effect of 5′-capping and the presence of the HCV 3′-UTR sequences on translation from an HCV IRES–luciferase fusion, we injected capped and uncapped transcripts either lacking a 3′-UTR, or containing the complete HCV 3′-UTR or a poly(A) tail into mice (Fig. 6B). Names of constructs containing a cap, HCV 3′-UTR, or poly(A) tail start with "Cap" or end with "3′-UTR" or "PolyA," respectively. The HCV 3′-UTR does not contain a poly(A) tail; however, a construct with a poly(A) tail was included to determine if the HCV 3′-UTR and a poly(A) tail were interchangeable. In all IRES experiments, values are reported as percentage

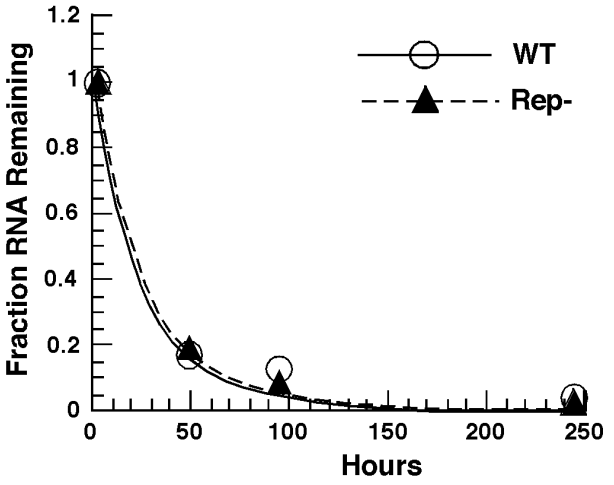

FIG. 5. Transduced genomic RNA does not replicate in mouse liver. The amount of injected HCV genomic RNA and rep⁻ RNA remaining at various times was measured using a quantitative RT-PCR assay. Measurements of HCV RNAs were normalized to measurements of human FIX produced from coinjected human FIX RNA and measurements of endogenous GAPD RNA. The rate of decay of HCV genomic RNA and rep⁻ RNA in mouse liver is similar, with a $t_{1/2}$ of ~ 22 hours, indicating that HCV genomic RNA does not replicate in mouse liver.

activity compared with HCV 3′-UTR (n = 10 for studies with HCV3′UTR, HCVpolyA, and HCVNoUTR; n = 5 for all remaining variants).

In mice, HCV3′UTR, HCVpolyA, and CapHCVPolyA expressed similar levels of luciferase, but expression from CapHCVNoUTR and HCVNoUTR RNA was low. The translational activity of CapHCV3′UTR was 68% of that of HCV3′UTR. Animals that received HCVPolyA, HCV3′UTR, CapHCVPolyA, and CapHCV3′UTR were imaged again at 24 hours and had approximately 4%, 4%, 7%, and 7%, respectively, of their original activity. From this, we can estimate that CapHCVPolyA and CapHCV3′UTR have similar stabilities, as do HCVPolyA and HCV3′UTR. Capped transcripts appeared to be slightly more stable than uncapped transcripts. The lack of expression from HCVNoUTR and CapHCVNoUTR may be due to RNA instability or an enhancement of translation by the 3′-UTR.

The effect of a cap and 3′-UTR was different in the three model systems. Both HeLa cells and mice required a poly(A) tail or HCV 3′-UTR for efficient translation (or RNA stability), but RRLs did not. Without a cap, HCV3′UTR and HCVPolyA translated equally well in mice, HeLa cells, and RRLs. Addition of a cap to HCVPolyA did not affect translation in mice. In contrast, the cap increased translation in HeLa cells and decreased translation in RRLs (270% and 50%, respectively). The presence of a cap decreased translation of CapHCV3′UTR in mice, HeLa cells, and RRLs to 68%, 24%, and 38%, respectively. This suggests that (1) a 3′-UTR is required for efficient translation or RNA stability in mice and HeLa cells but not in RRLs, (2) a cap and poly(A) tail synergistically enhance translation in HeLa cells, and (3) a cap inhibited translation in the context of the HCV 3′-UTR. All remaining IRES studies were conducted with uncapped RNAs ending in the HCV 3′-UTR, to mimic translation from the viral RNA.

Effect of Start Codon Mutations on Translation from the HCV IRES

Several reports showed that initiator codons other than AUG were functional in the context of the HCV IRES. A UUG codon has been shown to be functional in cell lysates and Huh-7 cells [34]. Studies in RRLs had indicated that IRESs with CUG and AUU start codons retained 90% activity [35].

To see if start codons other than AUG could be used in mice, we tested the variants CUG3′UTR and GUG3′UTR (AUG→CUG or GUG, respectively; Figs. 6A and 6B). In mice and HeLa cells, significant translational reductions were observed with CUG3′UTR (22% and 9.9%, respectively) and GUG3′UTR (19% and 7.8%, respectively). A CUG or GUG codon decreased translation to a lesser degree in RRLs (58% and 62%, respectively). These data suggest that mutations of the initiator codon are poorly tolerated *in vivo*, and RRLs have less stringent initiator codon requirements compared with HeLa cells and mice.

Effect of Internal Bulge Mutation of Domain IIId

Domain IIId has been shown to be critical for IRES function [13,36–40]. Most substitutions in this domain result in drastic reductions in translation *in vitro* and in culture, although some substitutions result in reductions of only 50–60%. The variant, IIId3′UTR, contained mutations in the internal bulge of IIId, which forms a loop E motif, a common stable RNA fold (Fig. 6A, legend) [41]. Mutations in the loop E motif of domain IIId resulted in activities of 41%, 3.4%, and 59%, respectively, in mice, HeLa cells, and RRLs (Fig. 6B). Thus some perturbation of the loop E motif in domain IIId is tolerated in mice and RRLs but not in HeLa cells.

Domains II and III Are Essential for Translation

We measured translational activities in mice for several deletion mutants Del(II)3′UTR, Del(IIIb)3′UTR, Del(II+IIIb)3′UTR, Del(IIa–IIIc)3′UTR, Del(IIa–IIId)3′UTR, which lacked domains II, IIIb, II and IIIb, II through IIIc, and II through IIId, respectively (Figs. 6A and 6B). Deletion of domains II and IIIb reduced translation to 2.7% and 20%, respectively. Deletion of domains II and IIIb, II through IIIc, and II through IIId decreased activity to 2.9%, 0.28%, and 0.40%, respectively.

We saw similar trends in the three model systems with all the large deletion mutants, except Del(IIIb)3′UTR. In all cases, RRLs showed the smallest decrease in translation, indicating that this system is the least stringent. Deletion

doi:10.1006/mthe.2002.0600, available online at http://www.idealibrary.com on IDEAL

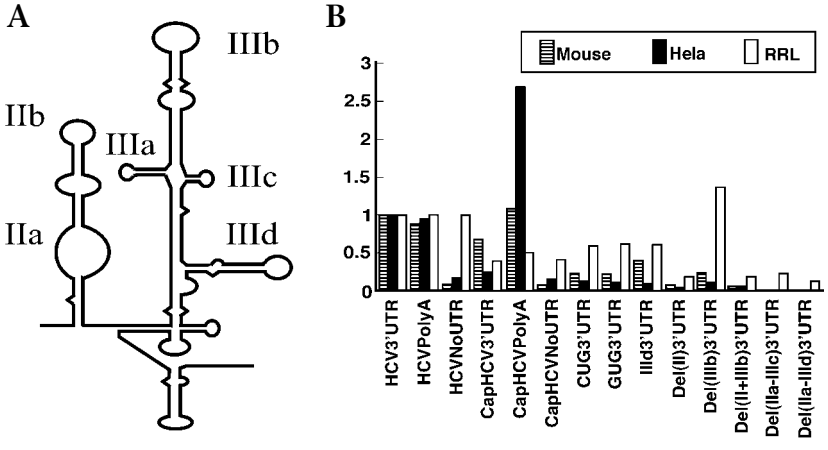

FIG. 6. Signal intensity depends on the presence of and identity of the 5′- and 3′-UTRs. Luciferase activity following injection of 40 μg of various IRES–luciferase fusions mixed with 40 μg of competitor RNA, 800 units of RNasin, and 2 ml of PBS at 25°C is shown. Numbering and IRES secondary structure based on Honda *et al.* [49]. IRESs comprise nucleotides 18–374. Names of constructs with a cap begin with "Cap". Names of constructs with wild-type IRESs begin with "HCV." CUG3′UTR and GUG3′UTR constructs have CUG and GUG initiator codons, respectively. CUGIIId3′UTR has an A residue inserted after nucleotides 274 and an A→U substitution at nucleotides 276. In Del(IIIb)3′UTR, nucleotides 178–221 were replaced with 5′-GGCCGAAAGGCC-3′. In the variants Del(II+IIIb)3′UTR, Del(IIa–IIIc)3′UTR, and Del(IIa–IIId)3′UTR, domain II was replaced with the sequence 5′-GGACTTCGGTGC-3′ and domains IIIa, IIIb, and IIIc or IIIa, IIIb, IIIc, and IIId, respectively, were replaced with the sequence 5′-CTTCGG-3′, 5′-CTTCGG-3′, or 5′-GGCCGAAAGGCC-3′, respectively. (A) Schematic of HCV IRES domain structure. Domains that were deleted in variants are indicated in parentheses within construct names. (For example, Del(II+IIIb)3′UTR indicates deletion of domains II and IIIb in a construct ending in the HCV 3′-UTR. Del(IIa–IIIc)3′UTR indicates deletion of domains IIa, IIb, IIIa, IIIb, and IIIc in a construct ending in the HCV 3′-UTR.) (B) Luciferase activity of wild-type and variant IRES–luciferase fusions in mice, HeLa cells, and nuclease-treated RRLs (number of animals ranged from 5 to 10). Error bars indicate SEM calculated for each group.

of domain II (Del(II)3′UTR) resulted in activities of 2.7%, 1.4%, and 11% in mice, HeLa cells, and RRLs, respectively. Deletion of domain IIIb resulted in activities of 20%, 6.1%, and 140% in mice, HeLa cells, and RRLs, respectively. Deletion of domains II and IIIb, domains II through IIIc, or domains II through IIId drastically reduced translation in mice and HeLa cells and to a lesser degree in RRLs. These results indicate that domains II and III are critical to IRES function.

The activity increase in RRLs upon deletion of domain IIIb was surprising, because IIIb comprises the eukaryotic initiation factor-3 (eIF3)–binding site [37,42]. The 40S ribosomal subunit binds to the IRES in the absence of any other translational factors [43]. However, ribosomal 48S complex formation is enhanced by eIF3 and is absolutely required for 80S complex formation on the HCV IRES. Binding studies as well as chemical and enzymatic protection studies indicate that eIF3 binds to domain IIIb [37,42], and deletion of IIIb abrogates eIF3 binding [42]. Previously, Honda *et al.* [13] reported that domain IIIb was required in RRLs, but their deletion mutant did not include a tetraloop sequence to promote proper folding.

The above results indicate that translational regulation in mice and HeLa cells was similar. RRLs seemed to have more relaxed translational regulation, although for gross mutations, trends were similar to those observed in mice and HeLa cells. There are, however, some interesting differences between the model systems that could provide the basis for further studies. We conclude that IRES RNAs introduced into the livers of mice by hydrodynamic RNA transfection show relevant translational regulation. Therefore, the mouse model system described here is suitable for the assessment of HCV translational inhibitors *in vivo*.

DISCUSSION

Development of novel therapeutics for the treatment of HCV has been hampered by the lack of small-animal model systems. In this study, we have attempted to develop a mouse model system to study HCV RNA translational regulation. Hydrodynamic RNA transfection allowed transfer of RNA to the cytoplasm of liver cells, the desired subcellular locale for HCV model studies. Translation of transfected RNAs was dependent on RNA dose.

We have demonstrated that the HCV IRES is functional in mouse liver. It is clear from our data that the lack of viral replication observed upon transfection with full-length HCV genomic RNAs is not due to a translational deficiency of the HCV IRES in mouse liver. Translation from the IRES in mouse liver did not require a cap, although a 3′-UTR greatly enhanced translation. Surprisingly, a poly(A) tail and the HCV 3′-UTR appeared to be functionally equivalent in translational enhancement. Domains II, IIIb, IIIa through IIIc, the AUG initiator codon, and to a lesser degree, a loop E motif in IIId, appeared to be important for efficient translation in mice.

Important differences in IRES-driven translation were observed in mice, HeLa cells, and RRLs. Translation from an uncapped IRES was dependent on the presence of a 3′-UTR in mice and HeLa cells but not in RRLs. The mouse and HeLa data are consistent with a model in which the IRES and the HCV 3′-UTR (or poly(A) tail) interact via RNA–protein interactions to circularize the RNA and facilitate ribosome reloading. However, we cannot exclude the possibility that the lack of translation from HCVNoUTR was due to RNA instability.

These three systems respond very differently to the presence of a cap and initiator codon mutations. Translation of HCVPolyA was not enhanced by capping in mice. A cap increased HCVPolyA translation in HeLa cells

by 2.5-fold or decreased it in RRLs by 50%. Capping decreased translation of HCV3′UTR in all three systems. Perhaps an interaction between the HCV 5′- and 3′-UTRs is interrupted by formation of a cap-binding complex. However, this does not explain the decrease in translation observed upon capping HCVNoUTR. CUG and GUG initiator codon mutations reduced IRES translation in RRLs by only 40%, but significantly decreased translation in mice and HeLa cells. Thus, an important proofreading step is not maintained in nuclease-treated RRLs.

In most cases, deletion and mutation of various domains of the IRES resulted in similar decreases in translation in mice and HeLa cells. A notable exception was the mutation of the internal loop of domain IIId. This variant was translated at reasonable levels in mice and RRLs but not in HeLa cells. As expected, deletion of domain IIIb, the putative eIF3-binding site, greatly reduced translation in mouse and in HeLa cells. This variant translated better than the wild-type sequence in RRLs. Of the three systems, RRLs showed the smallest translational response to all the mutations tested.

It is clear from our comparison of mice, RRLs, and HeLa cells that RRLs are translationally promiscuous. Ribosomal subunits and translational factors such as eIF2 and eIF3 may be present in excess of physiological levels in nuclease-treated RRLs as a result of the depletion of other mRNAs. This may lead to a loss of translational regulation in nuclease-treated RRLs. It is comforting that translational activity in HeLa cells largely correlates with translational activity in the liver of a mammal. Further work, however, will be required to determine why mice and HeLa cells respond differently to a cap and mutation of domain IIId.

As basic research into the mechanism of HCV IRES translational initiation progresses, novel inhibitors of HCV translation that target the IRES may be found. HeLa cell transfection will be a powerful tool to test these new approaches. However, before these new therapies are tested in humans, preclinical, small-animal model systems may serve to assess the efficacy, toxicity, and bioavailability of these new therapeutics. Many viruses of clinical and commercial importance, such as foot-and-mouth disease, rhinovirus, hepatitis A, and bovine viral diarrhea virus also utilize IRES elements. As suggested by the study of Chang *et al.* [21], hydrodynamic RNA transfection may be useful for development of small-animal models for these viruses.

Materials and Methods

Plasmids and transcripts. Capped and uncapped RNA transcripts were made by runoff *in vitro* transcription using a mMessage Machine or Megascript Kit, respectively (Ambion, Austin, TX) and treated with DNase I. RNAs were purified using a membrane that retains DNA (RNeasy Midi Kit; Qiagen, Germany). Transcripts and transcription templates are listed in the following format: RNA / transcription template (company if applicable) / runoff enzyme (or supercoiled) / polymerase. Luciferase RNA / pSP6controlDNA (Promega) / *Xmn*I / SP6; competitor RNA / pGEMEX-1 (Promega) / supercoiled / T7; antisense probe / pSP-luc+NF (Promega) / *Nhe*I / T7; sense probe / pSP-luc+NF (Promega)/ *Xho*I/SP6; HCVnoUTR / pHCVPolyA / *Bam*HI / T7; HCVPolyA / pHCVPolyA / *Xmn*I / T7; HCV3′UTR series / pHCV3′UTR / *Hpa*I / T7; FIXRNA / phFIX / *Xmn*I / SP6. The plasmid pWTHCV was created by amplifying the HCV IRES [44] by PCR using a primer containing a T7 promoter and inserting this fragment into the *Hin*dIII–*Nco*I sites of pGL3-Basic (Promega). The *Hin*dIII–*Xba*I fragment of the resulting plasmid was then ligated into pUC119. The plasmid pHCVPolyA was made by inserting the annealed primers 5′-CGAATTTTTTC(T_{30})G-3′ and 5′-GATCC(A_{30})GAAAAAATTCGGTAC-3′ into the *Bam*HI–*Kpn*I sites of pWTHCV. The plasmids used in Fig. 6 were made from pWTHCV by introducing the changes listed in the legend of Fig. 6 using a QuikChange mutagenesis kit (Stratagene, La Jolla, CA). The entire HCV 3′-UTR was amplified by PCR from the plasmid p90FLHCV [44] (from Charles Rice) with primers that contained the recognition sites for *Bam*HI and *Kpn*I. This fragment was inserted into the *Bam*HI–*Kpn*I sites of the plasmids generated using the QuikChange mutagenesis kit. The human FIX gene was amplified from pV4.1e-h.FIX [45] using the primers 5′-AATAATCTAGAGGGAAAGT-GATTAGTTAGTGAGA GGCCCTG-3′ and 5′-AATAACTGCAGCACCAT-GCAGCGCGTGACCATG-3′ and inserted as a *Pst*I–*Xba*I fragment into pSP64 poly(A) to make phFIX.

In situ hybridization and human FIX ELISA. Probes were made using a DIG RNA Labeling Kit (Roche, Indianapolis, IN). Light microscopy *in situ* hybridization was done on paraffin-embedded sections as described [44]. Electron microscopy *in situ* hybridization was done on glutaraldehyde-fixed and L.R. white-embedded sections and stained as described (http://biochem.roche.com/prod_inf/manuals/InSitu/InSi_toc.htm). Serum FIX levels were determined by ELISA as described [46].

Human FIX ELISA and quantitative RT-PCR. Serum FIX levels were determined by ELISA as described [46]. HCV RT-PCR was as described [47]. GAPD RT-PCR was done using rodent GAPD kit (PE Biosystems, Foster City, CA).

In vitro translation. We used 100 ng of capped or uncapped RNA to program RRLs (Promega), as recommended by the manufacturer, except that reactions were scaled to 12.5 μl. Products of the translation reaction were measured enzymatically using the luciferase assay system (Promega).

HeLa cell RNA transfections. After 2.5×10^5 cells were seeded in 35-mm plates and incubated overnight, 1 μg of capped or uncapped RNA was transfected using 10 μl Lipofectin (Gibco/BRL, Carlsbad, CA) as described [48]. Cells were pelleted 3 hours post-transfection, resuspended in 100 μl passive lysis buffer (Promega), and subjected to two cycles of freezing and thawing. Cellular debris was sedimented at 14,000*g* for 1 minute, and 20 μl of the supernatant was assayed using the luciferase assay system (Promega).

Injections and imaging. RNAs, RNasin, and competitor RNA were mixed, added to 2 ml of PBS, and steadily injected in the tail vein of mice over 4–5 seconds. Reproducibility of hydrodynamic transfection is highly dependent on the quality of injection and requires some practice. It is essential that the rate of injection be consistent from injection to injection. See Liu *et al.* [18] for a discussion of the parameters that influence hydrodynamic transfection. Animals that did not receive the entire volume in a single bolus were not imaged. At indicated times, 80 μl of 30 mg/ml luciferin was injected i.p. At 10 minutes postinjection, live anesthetized mice were imaged for 2 or 5 minutes. An intensified charge-coupled device (CCD) camera (model C2400-32; Hamamatsu, Japan) was used as described [25]. Raw values are reported as relative detected light per minute, and standard errors are shown. We obtained 18- to 22-g female BALB/c or NOD/LtSz-*Prkdcscid* mice from Jackson Laboratory (Bar Harbor, ME). Animals were treated according to NIH Guidelines for Animal Care and the Guidelines of Stanford University.

Acknowledgments

We thank Ramona Gonzales (University of California, Berkeley), Christopher H. Contag, Stephan Yant, and Karla Kirkegaard (all from Stanford University) for critical review of the manuscript, and Charles Rice (Washington University) and Alexander Kolykhalov (Eli Lilly) for providing plasmids. This work was supported by NIH grants T32 GM07276, AI47365 (P.S.), and AI99007 (M.A.K), respectively, and the Hutchison Program for Translational Research, Stanford University. K.O. and P.J.L. were the recipients of post-doctoral fellowships from the Japan Society for the Promotion of Science and the Max Kade Foundation, respectively.

doi:10.1006/mthe.2002.0600, available online at http://www.idealibrary.com on IDEAL

RECEIVED FOR PUBLICATION OCTOBER 31, 2001;
ACCEPTED MARCH 18, 2002.

REFERENCES

1. Mitra, A. K. (1999). Hepatitis C-related hepatocellular carcinoma: prevalence around the world, factors interacting, and role of genotypes. *Epidemiol. Rev.* **21:** 180–187.
2. Christie, J. M., and Chapman, R. W. (1999). Combination therapy for chronic hepatitis C: interferon and ribavirin. *Hosp. Med.* **60:** 357–361.
3. Kolykhalov, A. A., Feinstone, S. M., and Rice, C. M. (1996). Identification of a highly conserved sequence element at the 3′ terminus of hepatitis C virus genome RNA. *J. Virol.* **70:** 3363–3371.
4. Tanaka, T., *et al.* (1996). Structure of the 3′ terminus of the hepatitis C virus genome. *J. Virol.* **70:** 3307–3312.
5. Ito, T., Tahara, S. M., and Lai, M. M. (1998). The 3′-untranslated region of hepatitis C virus RNA enhances translation from an internal ribosomal entry site. *J. Virol.* **72:** 8789–8796.
6. Bukh, J., Purcell, R. H., and Miller, R. H. (1992). Sequence analysis of the 5′ noncoding region of hepatitis C virus. *Proc. Natl. Acad. Sci. USA* **89:** 4942–4946.
7. Wang, Q. M., and Heinz, B. A. (2001). Recent advances in prevention and treatment of hepatitis C virus infections. *Prog. Drug Res.* **(Spec. No.):** 79–110.
8. Mercer, D. F., *et al.* (2001). Hepatitis C virus replication in mice with chimeric human livers. *Nat. Med.* **7:** 927–933.
9. Hellen, C. U., and Pestova, T. V. (1999). Translation of hepatitis C virus RNA. *J. Viral Hepat.* **6:** 79–87.
10. Rijnbrand, R. C., and Lemon, S. M. (2000). Internal ribosome entry site-mediated translation in hepatitis C virus replication. *Curr. Top. Microbiol. Immunol.* **242:** 185–116.
11. Borman, A. M., *et al.* (1997). Comparison of picornaviral IRES-driven internal initiation of translation in cultured cells of different origins. *Nucleic Acids Res.* **25:** 925–932.
12. Kamoshita, N., *et al.* (1997). Genetic analysis of internal ribosomal entry site on hepatitis C virus RNA: implication for involvement of the highly ordered structure and cell type-specific transacting factors. *Virology* **233:** 9–18.
13. Honda, M., *et al.* (1996). Structural requirements for initiation of translation by internal ribosome entry within genome-length hepatitis C virus RNA. *Virology* **222:** 31–42.
14. Honda, M., *et al.* (2000). Cell cycle regulation of hepatitis C virus internal ribosomal entry site-directed translation. *Gastroenterology* **118:** 152–162.
15. Kay, M. A., and Fausto, N. (1997). Liver regeneration: prospects for therapy based on new technologies. *Mol. Med. Today* **3:** 108–115.
16. Fausto, N. (2000). Liver regeneration. *J. Hepatol.* **32:** 19–31.
17. Zhang, G., Budker, V., and Wolff, J. A. (1999). High levels of foreign gene expression in hepatocytes after tail vein injections of naked plasmid DNA. *Hum. Gene Ther.* **10:** 1735–1737.
18. Liu, F., Song, Y., and Liu, D. (1999). Hydrodynamics-based transfection in animals by systemic administration of plasmid DNA. *Gene Ther.* **6:** 1258–1266.
19. Yant, S. R., *et al.* (2000). Somatic integration and long-term transgene expression in normal and haemophilic mice using a DNA transposon system. *Nat. Genet.* **25:** 35–41.
20. Chen, Z. Y., *et al.* (2001). Linear DNAs concatemerize *in vivo* and result in sustained transgene expression in mouse liver. *Mol. Ther.* **3:** 403–410.
21. Chang, J., *et al.* (2001). Replication of the human hepatitis delta virus genome is initiated in mouse hepatocytes following intravenous injection of naked DNA or RNA sequences. *J. Virol.* **75:** 3469–3473.
22. Wolff, J. A., *et al.* (1990). Direct gene transfer into mouse muscle *in vivo*. *Science* **247:** 1465–1468.
23. Edinger, M., *et al.* (1999). Noninvasive assessment of tumor cell proliferation in animal models. *Neoplasia* **1:** 303–310.
24. Contag, C. H., *et al.* (1995). Photonic detection of bacterial pathogens in living hosts. *Mol. Microbiol.* **18:** 593–603.
25. Contag, C. H., *et al.* (1997). Visualizing gene expression in living mammals using a bioluminescent reporter. *Photochem. Photobiol.* **66:** 523–531.
26. Budker, V., *et al.* (2000). Hypothesis: naked plasmid DNA is taken up by cells *in vivo* by a receptor-mediated process. *J. Gene Med.* **2:** 76–88.
27. Zabner, J., *et al.* (1995). Cellular and molecular barriers to gene transfer by a cationic lipid. *J. Biol. Chem.* **270:** 18997–19007.
28. DeLuca, M., and McElroy, W. D. (1974). Kinetics of the firefly luciferase catalyzed reactions. *Biochemistry* **13:** 921–925.
29. Kolykhalov, A. A., *et al.* (1997). Transmission of hepatitis C by intrahepatic inoculation with transcribed RNA. *Science* **277:** 570–574.
30. Tsukiyama-Kohara, K., *et al.* (1992). Internal ribosome entry site within hepatitis C virus RNA. *J. Virol.* **66:** 1476-1483.
31. Fukushi, S., *et al.* (1994). Complete 5′ noncoding region is necessary for the efficient internal initiation of hepatitis C virus RNA. *Biochem. Biophys. Res. Commun.* **199:** 425–432.
32. Ito, T., and Lai, M. M. (1999). An internal polypyrimidine-tract-binding protein-binding site in the hepatitis C virus RNA attenuates translation, which is relieved by the 3′-untranslated sequence. *Virology* **254:** 288–296.
33. Sachs, A. B., Sarnow, P., and Hentze, M. W. (1997). Starting at the beginning, middle, and end: translation initiation in eukaryotes. *Cell* **89:** 831–838.
34. Hwang, L. H., *et al.* (1998). Involvement of the 5′ proximal coding sequences of hepatitis C virus with internal initiation of viral translation. *Biochem. Biophys. Res. Commun.* **252:** 455–460.
35. Reynolds, J. E., *et al.* (1995). Unique features of internal initiation of hepatitis C virus RNA translation. *EMBO J.* **14:** 6010–6020.
36. Kieft, J. S., *et al.* (1999). The hepatitis C virus internal ribosome entry site adopts an ion-dependent tertiary fold. *J. Mol. Biol.* **292:** 513–529.
37. Odreman-Macchioli, F. E., *et al.* (2000). Influence of correct secondary and tertiary RNA folding on the binding of cellular factors to the HCV IRES. *Nucleic Acids Res.* **28:** 875–885.
38. Rijnbrand, R., *et al.* (1995). Almost the entire 5′ non-translated region of hepatitis C virus is required for cap-independent translation. *FEBS Lett.* **365:** 115–119.
39. Jubin, R., *et al.* (2000). Hepatitis C virus internal ribosome entry site (IRES) stem loop IIId contains a phylogenetically conserved GGG triplet essential for translation and IRES folding. *J. Virol.* **74:** 10430–10437.
40. Yen, J. H., *et al.* (1995). Cellular proteins specifically bind to the 5′-noncoding region of hepatitis C virus RNA. *Virology* **208:** 723–732.
41. Lukavsky, P. J., *et al.* (2000). Structures of two RNA domains essential for hepatitis C virus internal ribosome entry site function. *Nat. Struct. Biol.* **7:** 1105–1110.
42. Sizova, D. V., *et al.* (1998). Specific interaction of eukaryotic translation initiation factor 3 with the 5′ nontranslated regions of hepatitis C virus and classical swine fever virus RNAs. *J. Virol.* **72:** 4775–4782.
43. Jackson, R. J., Howell, M. T., and Kaminski, A. (1990). The novel mechanism of initiation of picornavirus RNA translation. *Trends Biochem. Sci.* **15:** 477–483.
44. White, P. M., and Anderson, D. J. (1999). *In vivo* transplantation of mammalian neural crest cells into chick hosts reveals a new autonomic sublineage restriction. *Development* **126:** 4351–4363.
45. Nakai, H., *et al.* (1998). Adeno-associated viral vector-mediated gene transfer of human blood coagulation factor IX into mouse liver. *Blood* **91:** 4600–4607.
46. Walter, J., *et al.* (1996). Successful expression of human factor IX following repeat administration of adenoviral vector in mice. *Proc. Natl. Acad. Sci. USA* **93:** 3056–3061.
47. Morris, T., Robertson, B., and Gallagher, M. (1996). Rapid reverse transcription–PCR detection of hepatitis C virus RNA in serum by using the *Taq*Man fluorogenic detection system. *J. Clin. Microbiol.* **34:** 2933–2936.
48. Novak, J. E., Jarvis, T. C., and Kirkegaard, K. (1996). Techniques in molecular virology. In *Virology Methods Manual* (B. W. J. Mahy, Ed.), pp.165–185. Academic Press Ltd., New York.
49. Honda, M., Brown, E. A., and Lemon, S. M. (1996). Stability of a stem-loop involving the initiator AUG controls the efficiency of internal initiation of translation on hepatitis C virus RNA. *RNA* **2:** 955–968.